Quantum Dots Based *in-Vitro* Co-Culture Cancer Model for Identification of Rare Cancer Cell Heterogeneity

Satyanarayana Swamy Vyshnava
Sri Krishnadevaraya University
Gayathri Pandluru
Sri Krishnadevaraya University
Dileep Kumar Kanderi
Sri Krishnadevaraya University
Shiva Prasad Panjala
Osmania University
Swathi Banapuram
Osmania University
Kameshpandian Paramasivam
The Ultra arts and Science College
Varalakshmi Devi Kothamunireddy
Sri Krishnadevaraya University
Roja Rani Anupalli
Osmania University
Muralidhara Rao Dowlatabad (rao.muralidhara@gmail.com)
Sri Krishnadevaraya University

Research Article

Keywords: Quantum dots, cancer model, cancer cell heterogeneity, key element, modern medicine, patients

Posted Date: November 2nd, 2021

DOI: https://doi.org/10.21203/rs.3.rs-1008696/v1

Version of Record: A version of this preprint was published at Scientific Reports on April 7th, 2022. See the published version at https://doi.org/10.1038/s41598-022-09702-y.

Abstract

Cancer cell heterogeneity (CCH) is a key element in understanding cancer progression and metastasis. CCH is one of the challenges in therapeutics and diagnostics stumbling block in modern medicine. An *in-vitro* model of co-culture systems of MCF-7, HeLa, HEK-293, with THP-1 cells showed the occurrence of CTCs like cells with EpCAM+ and other cancer cell heterogenetic types with the Quantum Dot antibody conjugates (QD^{Ab}). This in-vitro model study could provide insights into the role of rare cancer cells and heterogeneity in metastasis, as well as the severity of infections in these patients. We successfully reported the presence of CCH based on the fluorescence ratios of the co-culture cancer cells. These short-term mimic co-cultures give a compelling and quite associated model for estimating early treatment responses in various types of cancers.

Introduction

Metastasis cancers are the leading cause of mortality due to poor prognosis during the progression of the disease[1,2]. Previous research has suggested that CCH exists in cancer metastasis that invades the bloodstream after being disseminated from the primary site of infection[3,4]. Tumor cell heterogeneity, as well as tumour morphologic heterogeneity, which is at the heart of many tumour grading and prognostic classification systems, has recently received more attention[5]. Cell proliferation, immune infiltration, differentiation status, and necrosis can all differ between microscopy fields within a tumour[4,6]. Intra-tumor heterogeneity and inter-tumor heterogeneity, among other molecular, phenotypic, and functional characteristics, can obstruct diagnosis and pose therapeutic challenges in bone, lung, brain, and liver cancer metastasis, these reports suggest that there is currently no systematic and comprehensive assessment of the molecular makeup of metastases[7]. Few reports have demonstrated the existence of phenotypically different subpopulations of tumorigenic and non-tumorigenic cells in various human malignancies, including acute myeloid leukaemia[8,9], chronic myeloid leukaemia[10,11], breast cancer[12,13], glioblastoma[14,15], colorectal cancer[16,17], pancreatic cancer[18,19], and ovarian cancers[12,20].

Multiple heterogenic cancer cells, such as epithelial to mesenchymal transition (EMT) cells and circulating tumor cells (CTCs), implying that the biological characteristics of individual CTCs, in addition to their number, should be taken into account[13,21]. CTCs are involved in distant metastasis, drug sensitivity, and apoptosis resistance[13,22,23]. Despite this, the majority of tumour cells die during transit due to biological and physical constraints such as shear stress and immune surveillance (apoptosis and anoikis), and only a small subset of surviving CTCs (approximately 0.01 percent) develop tumor-initiating cell potential[24,25].

The molecular basis of CTCs started with enriched fractions that made available only a limited amount of information on tumor heterogeneity[3,26]. Due to recent advances in single-cell technologies, CTC-specific genetic mutations have been discovered, and stereotyping of the CTC population has revealed the emergence of subclones with vibrant phenotypic traits that contribute significantly to the evolution of

the tumour genome during disease progression and treatment[22,25]. The clinical significance of the CTCs detected with the CellSearch® system removes only the majority of leukocytes by immunomagnetic enrichment of cells using epithelial cell adhesion molecule (EpCAM) antibodies coupled to ferrofluids, which lack of immunological marker like CD45[27]. Here in the present study, we isolated the CTCs with morphological characteristics such as having a nucleus and absence of cell surface marker CD45 in a co-culture of breast, cervical and renal cancer cell lines with monocytes through an *in-vitro* approach.

Methods

Materials. Chemicals as listed, Cadmium Oxide-99% (CdO), Zinc Acetate-99% (Zn(Act)2), Oleic Acid (OA), Sulfur powder-99% (S), Diphenylphosphine 98% (DPP), Trioctylphosphine 97% (TOP), Tetra-methyl-ammonium-hydroxide Solution (TMAH), N-hydroxy-succinimide-98% (NHS), NH2-(PEG)8-Propionic acid (nPEGc) are purchased from Sigma-Aldrich, 1-Octadecene-90% (ODE) purchased Acros Organics, Chloroform, Acetone, Methanol, Isopropanol (ISP) obtained from J.T.Baker, 3-Mercaptopropionic acid ≥99% (MPA) obtained from Merckmillipore, 1-ethyl-3-[3-dimethylaminopropyl] carbodiimide-98% (EDC) brought from Tokyo Chemical Industry Co, and Streptavidin (SA) purchased from Alfa Aesar.

Quantum dots synthesis. CdSe/ZnS/ZnS with OA capping are prepared as described in the established protocoll[28,35] nd labelled as QD^{450}, CdSe/ZnS with DPP as capping agent are prepared as described with minor changes in the synthesis process[28,36] and labelled as QD^{525}, CdSe/ZnS with TOP capped QDs are prepared as described with minor changes in the synthesis process[37–39] and labelled as QD^{615}. To make QDs for bio application, the surface of the QDs is modified through ligand exchange by MPA following conjugation with nPEGc and SA modifications with EDC/NHS coupling as mentioned in the previous reports[28]. The QDs with nPEGc-SA are purified by dialysis to remove any free/excess nPEGc and SA. The synthesized QDs are characterized for the fluorescence and absorbance efficacy with UV-Visible Spectroscopy.

Conjugation of antibodies to quantum dots. To conjugate, the antibodies (Abs) on the surface of QDs, antibodies Anti-EpCAM, Anti-CD45, and AntiCD44 are purchased from Thermofisher Scientific Inc. and Sigma Aldrich which are biotin coupled Abs. All the Abs are stored at -20^{o}C to extend their half-life. EDC, NHS, and MES are purchased from SRL.ltd and Sigma-Aldrich. QDs are primarily modified with MPA ligand exchange for the active $-COO^{-}$ group the QD_{MPA} (Quantum dots with MPA ligand) are then activated with EDC/NHS reaction as SA conjugation. To achieve successful conjugation of the Abs on the surface of QDs, an equimolar mixture of 1mM solution of EDC and NHS were prepared in the MES buffer at 4^{o}C (all the reaction are to be worked under the chilling condition to maintain the integrity of the Abs). 1mg of the individual QD_{MPA} are measured and dissolved in Millipore water, followed by the addition of the 200µL of EDC and the reaction was kept at 37^{o}C for 15 minutes followed by the addition of 200µL of NHS for 15 minutes to form an unstable intermediate compound of active carboxylic group facilitate to form a peptide bond with streptavidin. 1 µg/lit of SA was added to the above solution and allowed to form a strong $QD_{MPA/SA}$ (Quantum dot with streptavidin). The purified QDs which contain the SA is

allowed to react with Abs with biotin moiety to form strong biotin-streptavidin bonding. To made code for specific Abs, QD^{450} was bind with Anti-EpCAM (QD^{450}_{EpCAM}), QD^{525} was bind with Anti-CD45 (QD^{525}_{CD45}), and QD^{615} bind with Anti-CD44(QD^{615}_{CD44}). These QDs are subjected to purification by simple dialysis through dialysis cassettes. Later all the QDs are stored under the freezing condition to enhance the shelf life of the QD^{Ab}.

Cell culture and cytotoxicity. MCF-7, HeLa, cell lines are aquired from the National Centre for Cell Science (NCCS, Pune, India) while HEK-293, and THP-1 are brought from Bioresource Collection and Research Center (BCRC, Hsincchu, Taiwan). These cell lines were cultured in Dulbecco's modified Eagle's medium (DMEM), supplemented with 10% fetal bovine serum (FBS), 1 mg/ml glutamine and 100 µg/ml Streptomycin/Penicillin solution at 37^{o}C in a humidified atmosphere with 5% CO_2. For cytotoxicity assays, 12 mM 3-(4,5-Dimethylthiazol-2-yl)-2,5-Diphenyl tetrazolium Bromide (MTT) and sodium laurilsulfate (SDS) stock solutions were prepared according to manufacturer's instructions and stored at 4°C protected from light. Indivual cells were seeded in the population of 1×10^4 cells/ml in the 96 well flat bottom microtiter plates for an overnight before adding the QD_{MPA}. The desired amount of individual stock QD_{MPA} with concentrations of 0.1, 1, 5,10, 25, 50, and 100 µg/mL was dissolved in the MEM media (without phenol and Fetal bovine serum). 100 µl of each stock solution was added to the respective wells in the microtiter plates of the MCF-7, HeLa, HEK-293, and THP-1cells. These cells were cultured at optimal growth conditions for 24 h. To determine the viability of the cells, 10 µl of the MTT-PBS solution was added and the solution was incubated for 4 hrs. Subsequently, 100 µl SDS-HCl solution was added to the respective wells to dissolve the formazan crystals formed from the viable cells. Optical absorbance was read at 570 nm to quantify the MTT that reacted with the viable cells on a multi-plate reader (Multiskan Go, Thermo Scientific and µQuant, Bioteck).

Co-Cultures. THP-1 cells were plated in 6-well culture dishes, and various numbers of cancer cells (MCF-7, HeLa, and HEK-293) were introduced to the THP-1 plates, as shown in table S2. After 6 hours, cells were treated with three QDs specific to EpCAM, CD45, and CD44 Abs coupled QDs at predetermined concentrations. After 24 hours of exposure, cell viability and QD-specific binding were evaluated. Confocal imaging and flow cytometry analysis are used to depict the co-culture procedure.

Confocal microscopy. Compatibility of the QDs with the HeLa, MCF-7, HEK-293 and THP-1 cell lines, cellular imaging of the QDs uptake was studied when the individual cell lines attain 60-80% confluence of the cells was observed, followed by seeding on the coverslips $1x10^6$ cells per well. Allow to settle for 24 hrs, observe the health and confluence of the cells, then wash the cells with 1x PBS twice or thrice. Add fresh 1mL of media dispersed with QDs, the dilutions, and the concentrations. Allow the cells incubated for 20 minutes followed by washing the cells with 1x PBS twice or thrice, add 1x PBS, observe the cells under microscope with magnifications 10X, 40X, and 60X using the interface software Olympus flow view FVW-ASW to adjust the intensity of the lasers of the Confocal microscope (Olympus FV1000). Note the exposure time and the intensity plots of the cells, capture the pre processed image (RAW) for further processing. Store the cells with 95% paraformaldehyde or methanol for future usage.

Flow cytometry assay. In all experiments, each co-culture combination was seeded into a 12-well plate at $1x10^6$ cells/well for the flow cytometry assay. The cells were left to incubate for 24 hours. The culture media was replaced, and the prepared respective QDs solution was incubated into the wells at various concentrations. After incubation, the cells were rinsed with 1X PBS and left to settle for 5 minutes before being treated with EDTA solution, which is less damaging to cells than trypsin. After being fixed with 3% formaldehyde, the cells were suspended in 1x PBS. The fluorescence intensity of respective QDs binding was then evaluated using a multi-laser flow cytometry assay (BDTM LSR II, USA).

Statistical modeling. For statistical analysis, GraphPad Prism 5 (GraphPad Software, USA) and Origin 8.0 (OriginLab, USA) was employed. The mean standard deviation of three independent trails is then used to present all data. One-way analysis of variance was used to establish statistical significance, followed by a t-test. When $p > 0.05$, differences were deemed significant.

Results

Antibody conjugation with Quantum dots

The synthesized nPEGc functionalized quantum dots (QDs) include QD^{450}, QD^{525}, and QD^{615} based on respective fluorescence intensities were purified and made EDC/NHS coupling to provide an active amide bond between the QDs to the streptavidin[28]. The successful streptavidin conjugation with reference to the fluorescence intensities, respective QDs is represented in figure S1, where showed the relative fluorescence intensities of blue, green, and red hues. Antibodies include Anti-EpCAM, Anti-CD45, and Anti-CD44 which have biotin ends are allowed to couple with streptavidin-based QDs in a 1:1 ratio to maximize the coupling of the respective antibodies which are shown in table 1. The relative efficacy of the QDs was further analyzed with the cell culture preparations.

Binding Efficacy of the Antibody conjugated Quantum dots

To evaluate the binding efficacy of the QD^{Ab}, the cell lines are co-cultured to mimic peripheral blood samples. The standard culture conditions are maintained for optimal growth of the cell lines include MCF-7 (Human breast cancer cell line), HeLa (Human cervical cancer cell line), HEK-293 (Human embryonic kidney cell line), and THP-1(Human monocytic cell line). The QDs for respective normalized fluorescence intensity counts for specific above-mentioned cell lines are shown in table S1and figure S2. After 24 hours of cells incubation, aliquots of specific cell line groups are prepared followed by incubation of the QDs with incremental concentrations from 0.1 to 10 µg/mL. At higher concentrations of QDs i.e., of each aliquot for the specific cell lines as mentioned in figure S3, where MCF-7 cell lines show higher EpCAM+ at 10 µg/mL with lower cytotoxicity as shown in the supplementary figure S4. While HeLa and HEK-293 showed limited EpCAM+, while THP-1 cells are CD45+. For reference, all the cell lines are infested with CD44+ to represent the efficacy of the QD in the Co-Cultures to mention the heterogeneity of the cells.

Optimization of the Antibody conjugated Quantum dots

Aliquots of 5ml containing co-cultures of HeLa, MCF-7, and HEK-293 with THP-1 cells are allowed to grow for 24 hours under optimal conditions are observed for 90% confluency. These aliquots are pre-labeled for isolation of the EpCAM+, CD44+ and CD45+ cells lines using the flow cytometer. The set of prelabelled vials with MCF-7, HeLa, and HEK-293 are co-cultured with THP-1 cell lines are pre-stained with the blue, green, and red QDs. These are incubated for 15 minutes followed by washing twice or thrice with saline buffer and stored at lower temperatures before being subjected for sorting through flow cytometry. Using the standard designed protocol, the prelabeled vials containing cell lines are allowed to sort based on the fluorescence color intensities, using sterile vials cells are collected during sorting for further imaging. In evaluating the flow cytometry results as shown in figure 1, the contribution of the heterogeneity in the given *in-vitro* sample, the percentage of MCF-7 cell lines are more than the HeLa and HEK-293 cells with twice efficacy for EpCAM+/CD45+ and THP-1 cell for CD45+ with the reference to CD44+ for more than the EpCAM+ 9.45 ± 0.8%. The Sorted cell is subjected to imaging through confocal imaging, the sorted cells are observed with fine borders, showed healthier for a longer time with bright blue intensity for EpCAM+, green for CD45+ and bright red color for CD44+. figure 2 showed the histogram representation for the comparative heterogeneity of the MCF-7 cells with EpCAM+ and EpCAM- cells with CD45+ for THP-1 cells along with reference indicator CD44+. Based on figure 1, along with the binding efficacy, the heterogeneity was also determined based on the fluorescence ratio intensities, include blue: green: red (B: G: R) as shown in figure S5.

The capture of EpCAM+ and EpCAM- cells

Based on the optimized data of the QDs bindingefficacy, a series of trials are allowed to be designed for the capture of EpCAM+, CD45+ and CD44+ cells as shown in table S2. Each series are prelabelled for MCF-7, HeLa, HEK-293, and THP-1 which are co-cultured for 24 hours with optimal growth conditions. The trail I is assigned for the co-cultures of the MCF-7 and THP-1 cell lines showed a better affinity with 76% capture of EpCAM+ and CD45+ 78% and CD44+ 54% which is shown in figure 3a. Trail II is assigned for the co-cultures of the HeLa and THP-1 cell lines showed a better affinity with 62% capture of EpCAM+ and CD45 82% and CD44+ 68% which is shown in figure 3b. While trail III is assigned for the co-cultures of the HEK-293 and THP-1 cell lines showed a better affinity with 72% capture of EpCAM+ and CD45+ 82% and CD44+ 54% which is shown in figure 3c. Furthermore, we investigated the efficacy of the concept of capture the EpCAM+ and EpCAM- cell lines using QDs by multiple trials for each sample listed in table 2. Where we detected the possibility of finding each of the EpCAM+ will be a few events that were cross-checked with confocal imaging and flow cytometry sorting methods shown in figure S5. The events for EpCAM+ will be more effective for MCF-7 and HEK-293 rather than the HeLa cell lines co-cultures with THP-1.

Discussion

In our current study, the primary objective was to investigate the occurrence of rare cancer cells based on the specificity of the EpCAM+ and EpCAM- cell lines from *in-vitro* based blood mimic co-culture models. The goal was achieved successfully by showing the EpCAM+ cells in MCF-7, HeLa and HEK-293, and

EpCAM- for THP-1 cell lines (which are CD45+). Our cell line identification method enables us to provide the real-time assessment of the heterogeneity of the rare cancer cells in a given sample, which provides rapid detections of the EpCAM+ and EpCAM- cell lines. As metastasis progresses a few events such as EMTs are familiar from the recent publications which are considered to be EpCAM/CD44+[29] and EpCAM/CD45+[30], our approach suggested the existence of more CD44+ cells which is a well-known marker for EMT groups[31,32]. Meanwhile, some cells are positive for CD44/CD45+ which are more efficient in the metastasis EMT and MET (Mesenchymal to epithelial transition) groups[33,34].

We successfully demonstrated the *in-vitro* heterogeneity of the cancer cells when subjected to add QD^{Ab} with specific concentrations. The capture efficacy of the QDs was studied based on the standard plot was to check the required concentration of the QDs to be bound to the cell and optimization for the sorting the cells based on the respective fluorescence intensities through FACS (Fluorescence-activated cell sorting) as shown in the figure S5. CTCs identification in the current investigation is confined to EpCAM+ epithelial and mesenchymal cells. Given these constraints, we would expect $QD^{450/EPCAM}$ staining to compensate for EpCAM CTCs cells, in the case of epithelial CTCs. Total CTCs should be stained for EMT markers (CD44) in addition to $QD^{450/EPCAM}$ labeling because CTCs are escaping tumor cells derived from primary tumor tissue. These cells are more likely to be mesenchymal CTCs. Given the link between CTCs and recurrence in this study, we hypothesized that a QDs platform with staining for mesenchymal cancer markers (e.g., CD45/EpCAM and CD44/EpCAM) would be capable of more precise detection of CTCs via *in-vitro* multiplex staining for distinguishing epithelial and mesenchymal cancers. There was a significant difference in the EpCAM+ and EpCAM- groups in our sample ($p=0.001$, and $p=0.0001$) as shown in figure 3. However, by analyzing the type of cancer cells and co-cultures of recurrence, we were able to obtain meaningful data for the difference between the three cancer cell groups.

EpCAM+ cells were related with systemic pattern of recurrence in co-cultures, along with CD45+, CD44+, EpCAM/CD45+, EpCAM/CD44+, and CCD45/CD44+ with overall populations. These may be connected to the limitations of our investigation, which included a small number of cells and a short period of follow-ups. To raise the clinical value of EpCAM+ for cancer cells and validate the diagnostic capability of CTCs, one crucial component is the use of several antibodies to boost sensitivity and reduce CTC loss, followed by larger-scale research over a longer period. Finally, because CTCs are typically shed from tumor tissue, it is critical to examine the EMT/MET cancer stem cell markers status of CTCs in addition to tumor location. We believe that these findings will contribute to CTC research in different cancer investigations.

Conclusions

Our results demonstrated the availability of an efficient method for the analysis of metastasis progression by identification of rare cancer cell events include EMT, MET and CTC. The current protocol provided a successful assessment of rare cancer cell events based on the EpCAM+ and EpCAM- marker systems with more precision and accuracy. The results are cross-checked with similar trails with different

combinations for MCF-7, HeLa, HEK-293, and THP-1 cells. This principal method may help in delivering a new diagnostic approach in identifying the metastasis progression at the earlier prognosis of the disease.

Declarations

Acknowledgments

The authors sincerely acknowledge the financial support from the Indian council of medical research, New Delhi in the form of a Senior Research fellowship (ICMR File No. 5/3/8/81/ITR-F/2020-ITR). Advanced instrumentation was provided by the Centre for Nano and Soft Matter Sciences (CeNS), Bangalore. We also sincerely make our gratitude to mention the Department of Biotechnology, Sri Krishnadevaraya University for providing the immense resources and support to complete this research.

Author Contributions

The Concept and Design of this work were contributed by Mr. VSS; Dr. DMR and Prof. RRA provides the critical comments to complete this paper; The Data acquisition and scrutiny was contributed by Mr. KDK, Mrs. GP, Mr. SPP, Dr. KVD and Dr. SB; Manuscript proofreading was done by Dr. KPP.

Additional information

Supplementary Information was provided along with this article

Competing Interest

The authors state that they have no known competing financial interests or personal ties that may have influenced the work presented in this study.

References

1 van Dalum, G., Holland, L. & Terstappen, L. W. Metastasis and circulating tumor cells. *Ejifcc***23**, 87 (2012).

2 Brattain, M. G., Fine, W. D., Khaled, F. M., Thompson, J. & Brattain, D. E. Heterogeneity of malignant cells from a human colonic carcinoma. *Cancer research***41**, 1751-1756 (1981).

3 Meacham, C. E. & Morrison, S. J. Tumour heterogeneity and cancer cell plasticity. *Nature***501**, 328-337 (2013).

4 Dagogo-Jack, I. & Shaw, A. T. Tumour heterogeneity and resistance to cancer therapies. *Nature reviews Clinical oncology***15**, 81 (2018).

5 Kanzaki, R. & Pietras, K. Heterogeneity of cancer-associated fibroblasts: Opportunities for precision medicine. *Cancer Science***111**, 2708 (2020).

6 Guo, M., Peng, Y., Gao, A., Du, C. & Herman, J. G. Epigenetic heterogeneity in cancer. *Biomarker research***7**, 1-19 (2019).

7 Koren, S. & Bentires-Alj, M. Breast tumor heterogeneity: source of fitness, hurdle for therapy. *Molecular cell***60**, 537-546 (2015).

8 Thakral, D. *et al.* Real-time molecular monitoring in acute myeloid leukemia with circulating tumor DNA. *Frontiers in Cell and Developmental Biology***8** (2020).

9 Hughes, C. F., Gallipoli, P. & Agarwal, R. Design, implementation and clinical utility of next generation sequencing in myeloid malignancies: acute myeloid leukaemia and myelodysplastic syndrome. *Pathology* (2021).

10 Almshayakhchi, R. N. *HAGE and WT1 proteins as promising immunotherapeutic targets in chronic myeloid leukaemia*, Nottingham Trent University, (2020).

11 Habib, E. M. *et al.* Circulating miR-146a expression predicts early treatment response to imatinib in adult chronic myeloid leukemia. *Journal of Investigative Medicine***69**, 333-337 (2021).

12 Norouzi-Barough, L. *et al.* Early diagnosis of breast and ovarian cancers by body fluids circulating tumor-derived exosomes. *Cancer Cell International***20**, 1-10 (2020).

13 Yu, T. *et al.* Heterogeneity of CTC contributes to the organotropism of breast cancer. *Biomedicine & Pharmacotherapy***137**, 111314 (2021).

14 Krol, I. *et al.* Detection of circulating tumour cell clusters in human glioblastoma. *British journal of cancer***119**, 487-491 (2018).

15 Bark, J. M., Kulasinghe, A., Chua, B., Day, B. W. & Punyadeera, C. Circulating biomarkers in patients with glioblastoma. *British journal of cancer***122**, 295-305 (2020).

16 Dasari, A. *et al.* ctDNA applications and integration in colorectal cancer: An NCI Colon and Rectal–Anal Task Forces whitepaper. *Nature Reviews Clinical Oncology***17**, 757-770 (2020).

17 Pramil, E., Dillard, C. & Escargueil, A. E. Colorectal Cancer and Immunity: From the Wet Lab to Individuals. *Cancers***13**, 1713 (2021).

18 Navarro-Marchal, S. I. A. *et al.* Anti-CD44-conjugated olive oil liquid nanocapsules for targeting pancreatic cancer stem cells. *Biomacromolecules* (2021).

19 Sellahewa, R., Lundy, J., Croagh, D. & Jenkins, B. High circulating tumour DNA is a strong negative prognostic factor in operable pancreatic cancer. *HPB***23**, S263 (2021).

20 Tong, J. G. *et al.* Spatial and temporal epithelial ovarian cancer cell heterogeneity impacts Maraba virus oncolytic potential. *BMC cancer***17**, 1-13 (2017).

21 Shibue, T. & Weinberg, R. A. EMT, CSCs, and drug resistance: the mechanistic link and clinical implications. *Nature reviews Clinical oncology***14**, 611 (2017).

22 Batth, I. S. *et al.* CTC analysis: An update on technological progress. *Translational Research***212**, 14-25 (2019).

23 Zeinali, M. *et al.* High-throughput label-free isolation of heterogeneous circulating tumor cells and CTC clusters from non-small-cell lung cancer patients. *Cancers***12**, 127 (2020).

24 Zavridou, M. *et al.* Direct comparison of size-dependent versus EpCAM-dependent CTC enrichment at the gene expression and DNA methylation level in head and neck squamous cell carcinoma. *Scientific reports***10**, 1-9 (2020).

25 Tayoun, T. *et al.* CTC-derived models: a window into the seeding capacity of circulating tumor cells (CTCs). *Cells***8**, 1145 (2019).

26 Rushton, A. J., Nteliopoulos, G., Shaw, J. A. & Coombes, R. C. A review of circulating tumour cell enrichment technologies. *Cancers***13**, 970 (2021).

27 De Wit, S. *et al.* The detection of EpCAM+ and EpCAM−circulating tumor cells. *Scientific reports***5**, 1-10 (2015).

28 Vyshnava, S. S. *et al.* Gram scale synthesis of QD 450 core–shell quantum dots for cellular imaging and sorting. *Applied Nanoscience***10**, 1257-1268 (2020).

29 Marhaba, R. *et al.* CD44 and EpCAM: cancer-initiating cell markers. *Current molecular medicine***8**, 784-804 (2008).

30 Horikawa, M., Iinuma, H., Inoue, T., Ogawa, E. & Fukushima, R. Clinical significance of intraperitoneal CD44 mRNA levels of magnetically separated CD45-negative EpCAM-positive cells for peritoneal recurrence and prognosis in stage II and III gastric cancer patients. *Oncology reports***25**, 1413-1420 (2011).

31 Antony, J., Thiery, J. P. & Huang, R. Y.-J. Epithelial-to-mesenchymal transition: lessons from development, insights into cancer and the potential of EMT-subtype based therapeutic intervention. *Physical biology***16**, 041004 (2019).

32 Pastushenko, I. & Blanpain, C. EMT transition states during tumor progression and metastasis. *Trends in cell biology***29**, 212-226 (2019).

33 Bakir, B., Chiarella, A. M., Pitarresi, J. R. & Rustgi, A. K. EMT, MET, plasticity, and tumor metastasis. *Trends in Cell Biology* (2020).

34 Wilson, M. M., Weinberg, R. A., Lees, J. A. & Guen, V. J. Emerging mechanisms by which EMT programs control stemness. *Trends in cancer* (2020).

35 Hanmandlu, C. *et al.* Suppression of surface defects to achieve hysteresis-free inverted perovskite solar cells via quantum dot passivation. *Journal of Materials Chemistry A***8**, 5263-5274 (2020).

36 Hsia, C.-H., Wuttig, A. & Yang, H. An accessible approach to preparing water-soluble Mn2+-doped (CdSSe) ZnS (core) shell nanocrystals for ratiometric temperature sensing. *ACS nano***5**, 9511-9522 (2011).

37 Fournier-Bidoz, S. *et al.* Facile and rapid one-step mass preparation of quantum-dot barcodes. *Angewandte Chemie International Edition***47**, 5577-5581 (2008).

38 Howarth, M. *et al.* Monovalent, reduced-size quantum dots for imaging receptors on living cells. *Nature methods***5**, 397-399 (2008).

39 Lim, S. J., Chon, B., Joo, T. & Shin, S. K. Synthesis and characterization of zinc-blende CdSe-based core/shell nanocrystals and their luminescence in water. *The Journal of Physical Chemistry C***112**, 1744-1747 (2008).

Tables

Table 1: Quantum dots coupled with antibodies, based on the requirement of the targeted cells

Quantum Dots	Antibodies	Conjugate	Targeted cells
$QD^{450/MPA}$	Anti-EpCAM	$QD^{450/EpCAM}$	Epithelial cells
$QD^{525/MPA}$	Anti-CD45	$QD^{525/CD45}$	Mesenchymal cells
$QD^{615/MPA}$	Anti-CD45	$QD^{615/CD44}$	Epithelia cells

Table 2: Cells captured when treated with respective Antibody Quantum dots Conjugates

QD_Ab Conjugates	Percentage of cells (%)		
	MCF-7	HELA	HEK-293
EpCAM+	9.45 ± 0.8	7.71 ± 0.9	8.84 ± 0.2
CD45+	3.76 ± 0.6	2.97 ± 1.0	4.77 ± 0.5
CD44+	3.25 ± 0.6	1.6 ± 1.0	2.03 ± 0.7
EpCAM/CD44+	4.79 ± 0.8	6.07 ± 0.3	6.21 ± 0.4
EpCAM/CD45+	2.86 ± 0.4	2.6 ± 0.5	3.13 ± 0.9
CD45/CD44+	1.5 ± 1.0	1.31 ± 0.9	1.62 ± 0.9

Figures

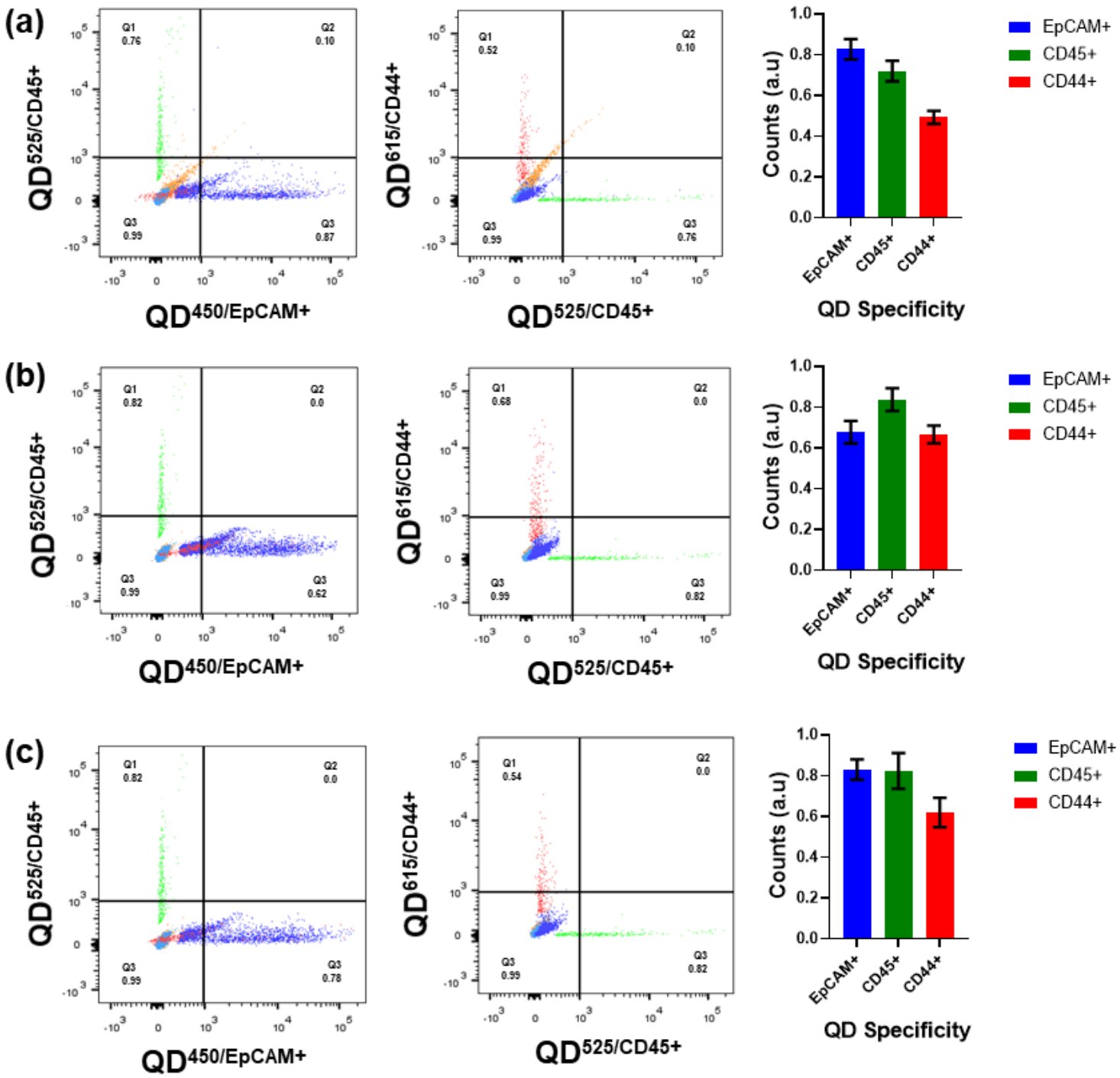

Figure 1

Flowcytometry dot plot images for capture the EpCAM+ and EpCAM- cells by using the quantum dot conjugated with anti-EpCAM, anti-CD45, and anti-CD44 cells in co-culture cells in in-vitro incubated with concentrations at 1.0 µg/5mL in 1x PBS media were analyzed through flow cytometry (a) MCF-7 and THP-1 (b) HeLa and THP-1 (c) HEK-293 and THP-1 cancer cell lines co-cultures with fluorescence emission and insight histograms show the flow cytometry with respective Quantum dots binding.

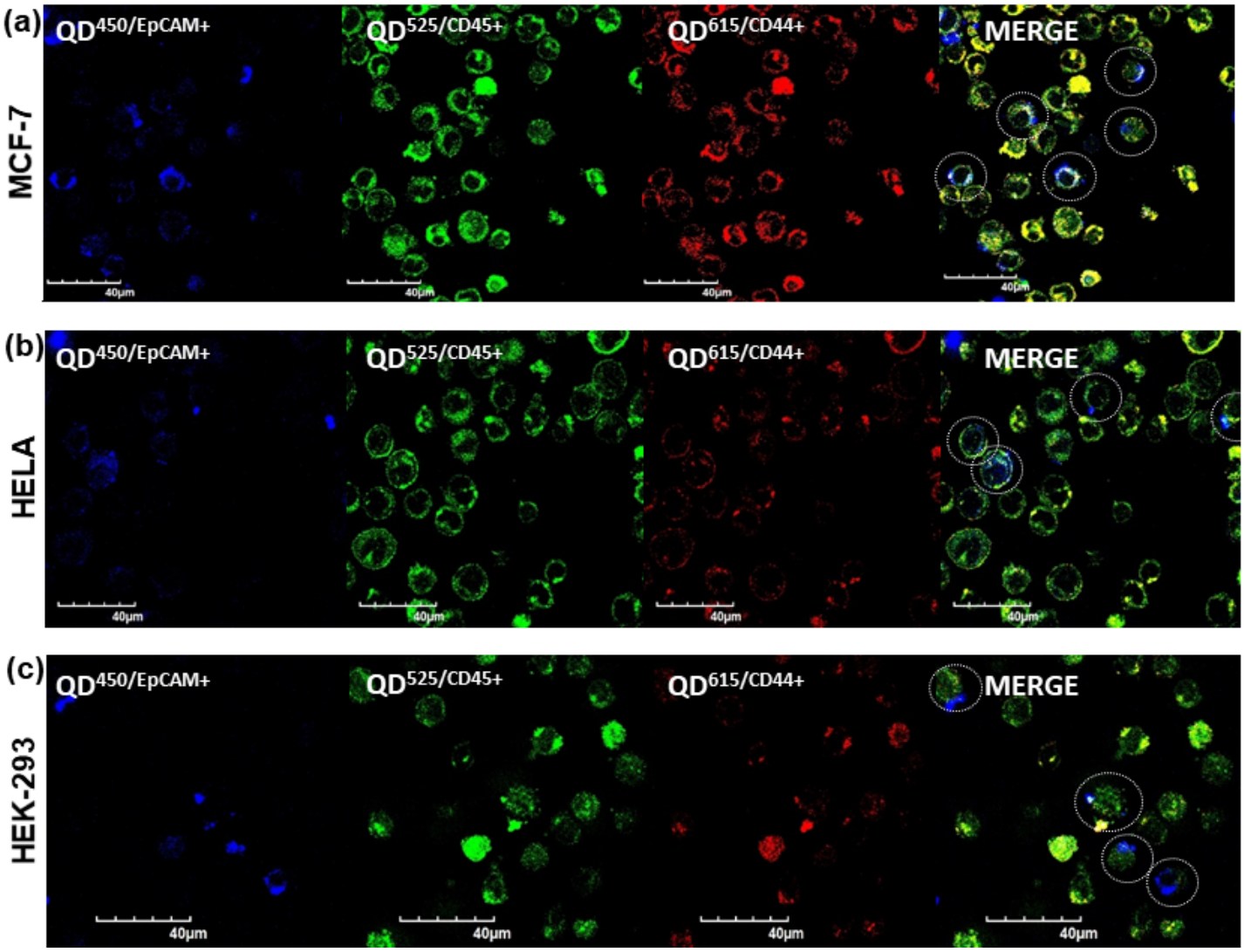

Figure 2

Confocal microscopic images for capture the EpCAM+ and EpCAM- cells by using the quantum dot conjugated with anti-EpCAM, anti-CD45, and anti-CD44 cells in co-culture cells in in-vitro incubated with concentrations at 1.0 µg/5mL in 1x PBS media were analyzed through confocal imaging (a) MCF-7 and THP-1 (b) HeLa and THP-1 (c) HEK-293 and THP-1 cancer cell lines co-cultures with fluorescence emissions shows the confocal images with respective Quantum dots binding, which are represented with dotted circles.

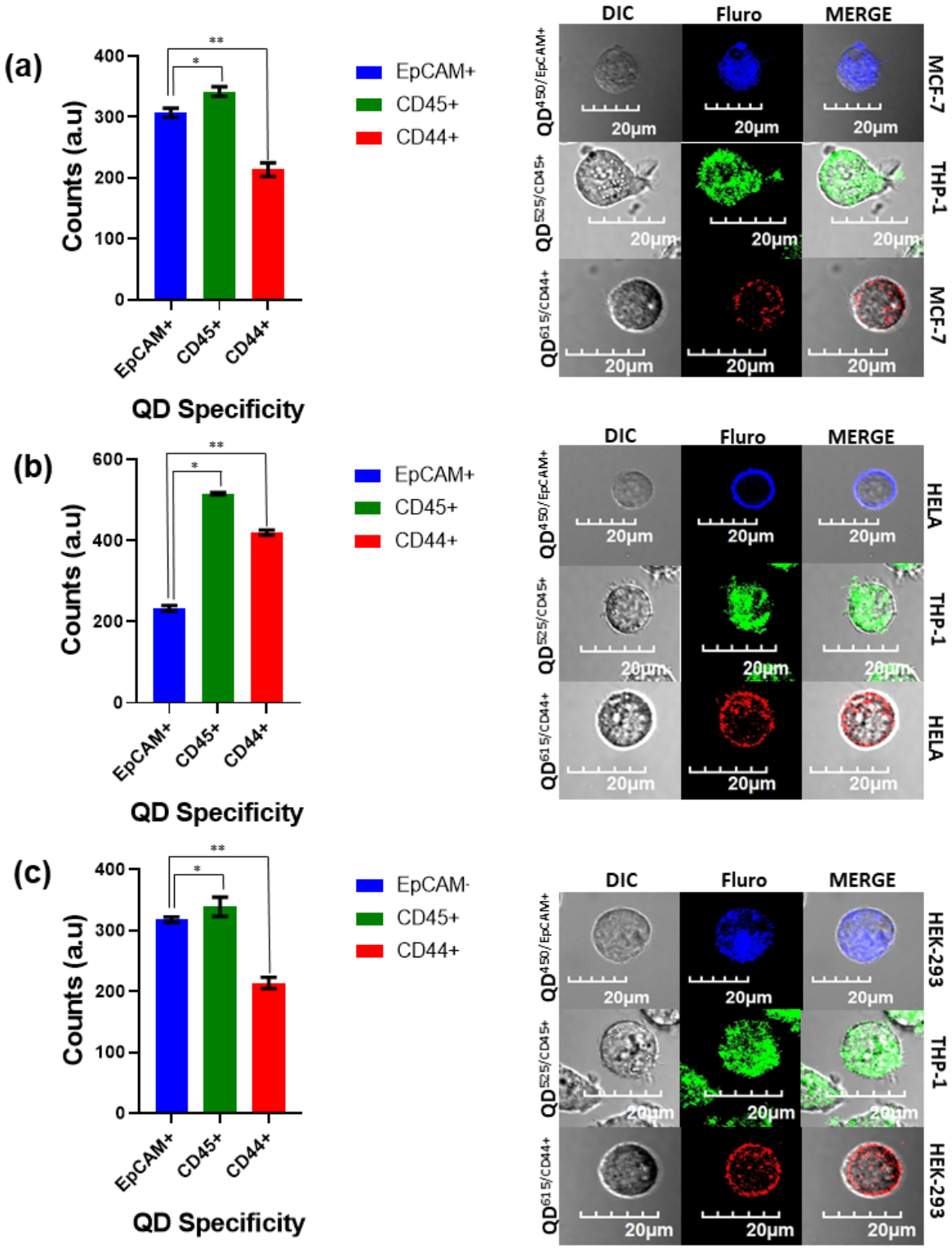

Figure 3

Multiple trails for each cell line in the co-cultures incubated with respective quantum dot antibody conjugates in-vitro with incubated with concentrations from 1.0 µg/5mL media for significant analysis through flow cytometry and confocal imaging (a) MCF-7, and THP-1 (b) HeLa, and THP-1 (c) HEK-293, and THP-1 and HeLa cancer cell lines co-cultures with respective fluorescence emission shows the quantum dots binding. The statical data shows the probability of the occurrence of the EpCAM+ and

EpCAM- cells, through reference through T-test was performed; “*” stands for the significance level <0.001, and “**” stands for the significance level <0.0001.

Supplementary Files

This is a list of supplementary files associated with this preprint. Click to download.

- Supplimentaryinformation.docx